Energy Conversion and Management 50 (2009) 539–542

Contents lists available at ScienceDirect

Energy Conversion and Management

journal homepage: www.elsevier.com/locate/enconman

Direct computation of ac machine inductances based on winding function theory

E.S. Obe *

Department of Electrical Engineering, University of Nigeria, Nsukka, Nigeria

ARTICLE INFO

Article history:
Received 8 April 2008
Accepted 28 October 2008
Available online 9 December 2008

Keywords:
Winding function
Inductances
Ac machines
Slots
Inverse airgap function
Synchronous reluctance machine

ABSTRACT

A numerical procedure for computing the inductances of ac machines is described. The procedure does not require that explicit expressions for airgap or winding functions be obtained therefore complicated integrations are avoided. The effects of stator slots are included in a manner in which all the harmonics are taken into account. The inductances obtained are subsequently transformed to *d*-*q*-0 reference frame and the results are seen to compare favorably with measurements. Significant differences exist in the computed inductances especially in the d-axis. Cross-coupling effects between the *d*-axis and *q*-axis inductances which are generally ignored when approximate expressions are used are also observed.

1. Introduction

The winding function (WF) theory developed in the early 1950s is a veritable tool for calculation of ac machine inductances [1,2]. The finite element (FE) method [3] though more accurate is cumbersome because it requires an extensive characterization of the machine studied, for example, the physical geometry, instantaneous winding current distribution, electromagnetic properties of all the materials making up the machine and an advanced knowledge of electromagnetic fields. Additionally, several boundary conditions must be specified before the model calculations can be performed. In this paper, it is shown that the WF method can by very simple numerical procedure, yield very accurate results even though the only information required are the winding layout and machine geometry. However, if more machine parameters other than inductances are required, FE may be a better option.

In traditional WF procedures, only the fundamental components of winding functions and only the average plus the second harmonic component of the inverse airgap functions are used. The expressions are so truncated because the known WF formula for calculating inductances requires that explicit expressions for the winding pattern and inverse gap function be obtained. These, coupled with the assumptions that the windings are placed in the periphery of the airgap whereas they are in slots, reduces the accuracy of the computed results. Even with such simplifications, the integrations to be performed can be challenging. After these, the inductance expressions so obtained in the *a*–*b*–*c* frame will be easy to transform to *d*-*q*-0 frame. However, the end results in the *d*-*q*-0 frame are not required in the form of expressions and therefore, the intermediate expressions obtained for the inductances in the *a*–*b*–*c* frame are not so useful.

The recent papers [4,5] on this subject modified the inverse airgap function with a model of the slots and skew and obtained excellent results that compare very favorably with the finite element solutions. Although they included the effect of slots, it appears that approximated Fourier series expressions were still used. This study emphasizes the need to use directly the actual machine geometry and winding placement positions to perform these calculations and not approximate expressions representing them. This will ensure that all space harmonics ignored by the Fourier series expressions are included in the results. In this paper, the calculation of inductances of a cageless rotor three-phase synchronous reluctance motor whose design data is shown in Table 1 is used to demonstrate the procedure.

1.1. The winding function

The WF theory [2] states that the inductance L_{XY} between any two windings X and Y is

$$L_{XY} = \mu_o rl \int_0^{2\pi} \left(\frac{N_X(\varphi)N_Y(\varphi)}{g(\varphi, \theta_r)} \right) d\phi \tag{1}$$

In (1) μ_o is the permeability of free space, r is the effective radius of the stator bore, l is the machine stack length, N_X and N_Y are the winding functions for windings X and Y, respectively, g is airgap function, φ is the stator circumferential position and θ_r is the rotor position.

* Tel.: +234 803 250 5664.
E-mail address: obeunn@yahoo.com

0196-8904/$ - see front matter © 2008 Elsevier Ltd. All rights reserved.
doi:10.1016/j.enconman.2008.10.017

Table 1
Machine dimensions.

Quantity	Value
Stator outer/inner radius	105.02/67.99 mm
Rotor radius	67.69 mm
Effective stack length	160.22 mm
Number of slots	36
Number of turns	32
Main airgap length g_1	0.4 mm
Inter-polar slot space g_2	21.3 mm
Stator slot depth	18 mm
Stator slot pitch	10°
Ratio pole arc/pole pitch	2/3
Number of poles	4
Winding connection	Y
Number of coil groups	2

Simplified expressions for the component parts of the right hand side of (1) will not be used here; rather their graphical representation will be shown and used to compute the inductances directly.

2. Inductance calculation procedure

For ease of discerning in the following discussions, the actual model refers to the real machine geometry and winding patterns and the approximate Fourier series models is termed the sinusoidal model. To account for slot openings, the values of airgap lengths used for the calculations in the sinusoidal model are corrected by Carter's curves to $g_1 = 0.47$ mm and $g_2 = 34.3$ mm while the values listed in Table 1 were used for the actual model calculations. The winding function for winding of phase A and the inverse airgap function for the machine under study are shown in Fig. 1. The dotted plots in Fig. 1a and b represent the sinusoidal winding function and the inverse airgap functions, respectively. They have the following forms:

$$N_X = \frac{4N}{\pi}\cos\left(\phi - k\frac{2\pi}{3}\right) \tag{2}$$

where $x = 0, 1, 2$ for phases A, B and C, respectively, and N is the number of turns per phase.

$$g^{-1}(\phi, \theta_r) = a - b\cos 2(\phi - \theta_r) \tag{3}$$

where $a = \frac{1}{2}\left(\frac{1}{g_1} + \frac{1}{g_2}\right)$, $b = \frac{2}{\pi}\left(\frac{1}{g_1} - \frac{1}{g_2}\right)\sin\pi\beta$ and β is the ratio of pole arc to pole pitch.

It is seen in Fig. 1 that parts of the windings and the rotor are actually ignored if simplified expressions (2) and (3) are used.

The procedure adopted here is to model the entire stator slots and rotor as they are. The first step is to divide each stator slot into n elemental but equal areas to ensure accuracy. In this paper $n = 400$. Similar matching divisions are also made on the salient-pole rotor iron, which for this case a rotor pole pitch is divided into $9n$. The overall airgap function G (including the effect of slots), for a

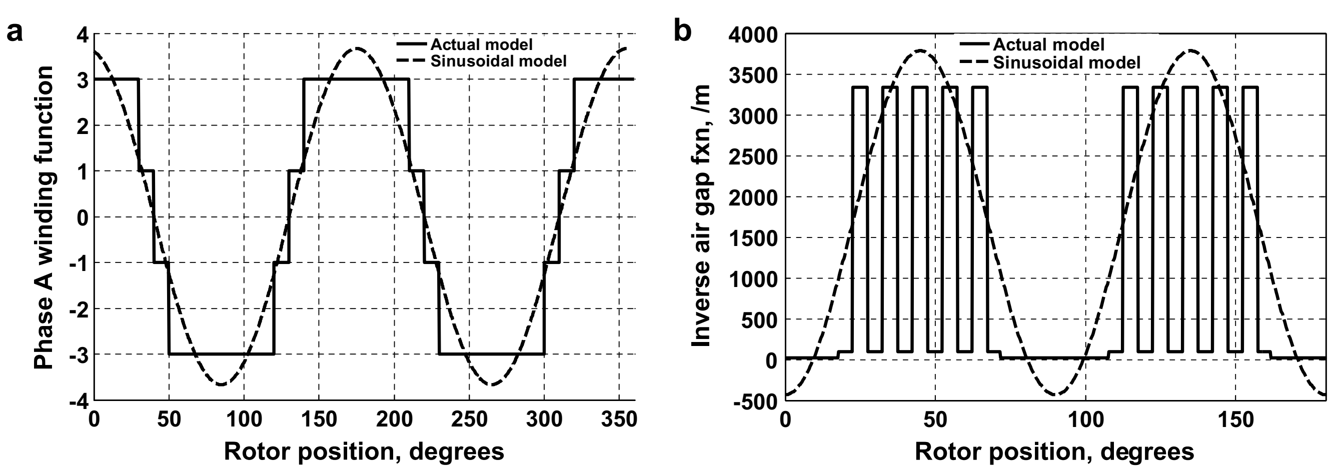

Fig. 1. Actual and sinusoidal models. (a) Winding functions (per turn). (b) Rotor inverse airgap functions (including the effects of saliency and slots).

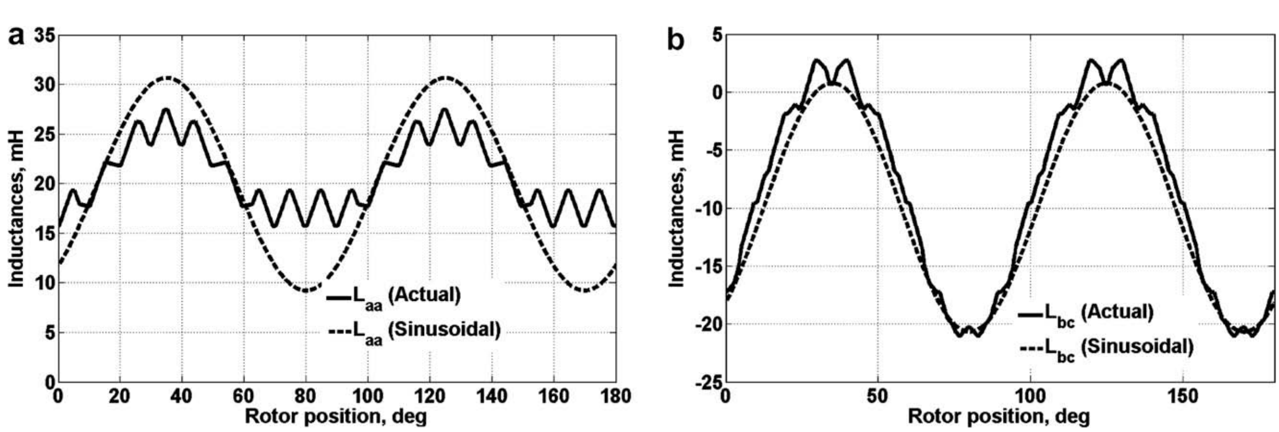

Fig. 2. Calculated inductances (a) self (b) mutual-inductances.

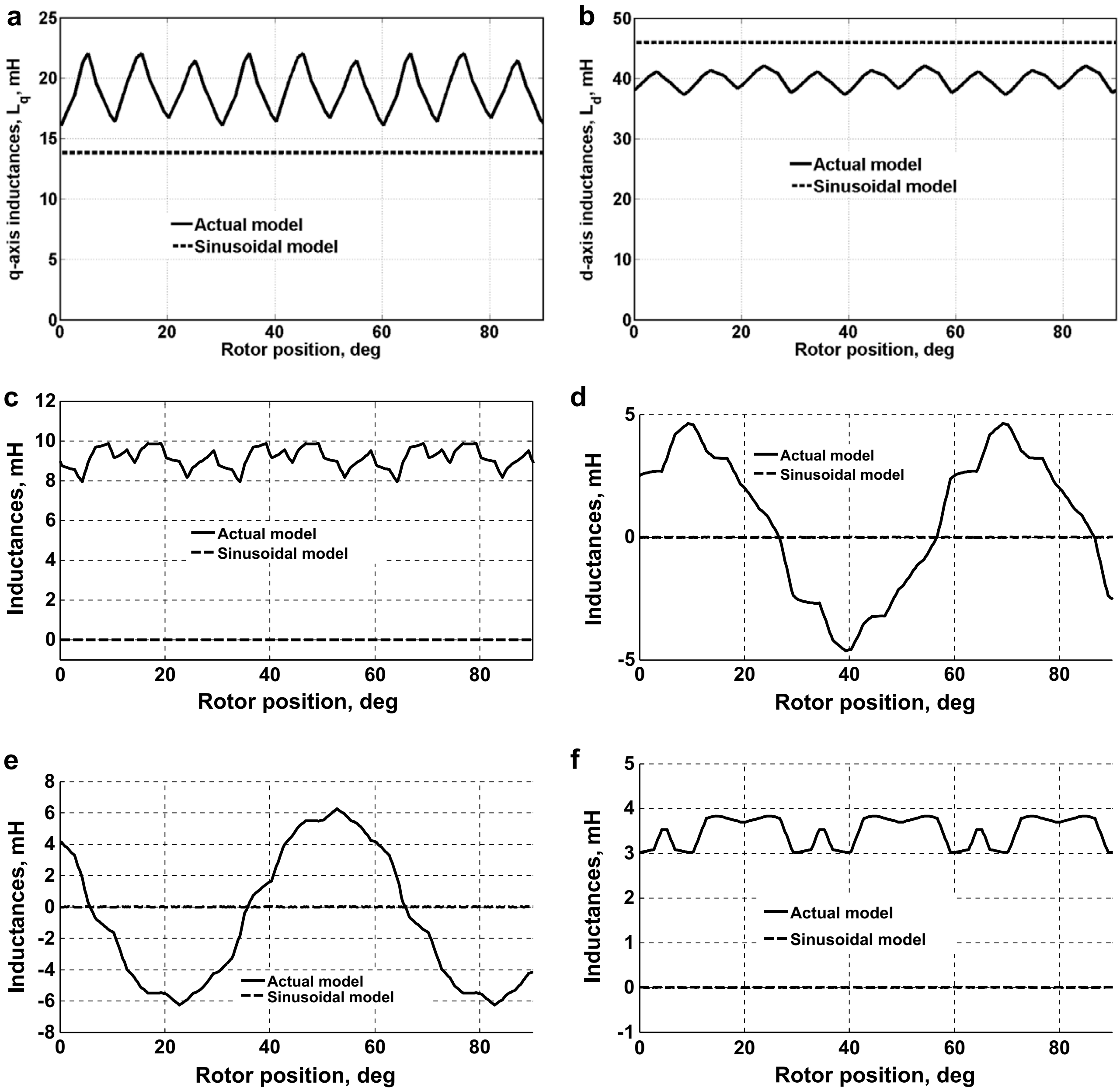

Fig. 3. Transformed inductances, (a) L_q, (b) L_d, (c) L_{dq}, (d) L_{0q}, (e) L_{0d}, and (f) L_{00}.

particular rotor position is obtained by geometrically adding the rotor gap function to the stator slot function as the rotor slides in n incremental steps from 0 to 2π mechanical radians. The stator slot function is held static all the time. The shape of this geometric sum changes for every nth change of rotor position but maintains the same area and that is what is 'seen' by the stator windings. The shape for an arbitrary rotor position is shown in Fig. 1b. For every change, this will be used for the computation of inductances which are stored as arrays. This computation procedure is performed for both the actual and the sinusoidal models simultaneously.

With the data for the winding patterns and effective airgap positions obtained for each step change, the computations for different inductances (self and mutual) are performed using the equation:

$$L_{XY}(j) = \mu_o rl\left(m\sum_{i=1}^{n}\frac{N(i)N(j)}{G(i,j)}\right) \quad (4)$$

where $G(i,j)$ is the effective airgap function including the slot effects and $m = \frac{2\pi}{n}$. This equation is very similar to (1).

The inductances computed by this procedure are shown in Fig. 2 where the effects of the slots are seen to be more pronounced in the self inductances. The presence of slots produces a waveform with frequency equal to the slot-pitch which modulates the inductance waveform.

3. Transformations to *d*-*q*-0 frame

In order to obtain the d-q-0 values of the inductances transformation to rotor reference frame using Park's transformation can be performed. The equation of transformation is

$$L_{d-q-0} = T(\theta_r)L_{abc}T(\theta_r)^{-1} \quad (5)$$

Table 2
Computed values of d-q-0 inductances (mH).

Parameter	Calculated (Sinusoidal)	Calculated (Actual)	Measured
L_d	49.953	39.682	41.04
L_q	13.807	18.645	19.13
L_{dq}	0.000	9.144	–
L_{00}	0.000	4.1143	–

where $T(\theta_r)$ is

$$T(\theta_r) = \begin{bmatrix} \cos\theta_r & \cos\left(\theta_r - \frac{2\pi}{3}\right) & \cos\left(\theta_r - \frac{4\pi}{3}\right) \\ \sin\theta_r & \sin\left(\theta_r - \frac{2\pi}{3}\right) & \sin\left(\theta_r - \frac{4\pi}{3}\right) \\ \frac{1}{\sqrt{2}} & \frac{1}{\sqrt{2}} & \frac{1}{\sqrt{2}} \end{bmatrix}$$

The plots of axis inductances obtained using (5) over one pole pitch is shown in Fig. 3. It is seen that ripples also exist in the inductances and this is still due to the effect of slots. The average values obtained from these calculations are compared with measured values are shown in Table 2.

4. Conclusions

Significant differences exist between the two computed values especially in the d-axis inductances because the effect of slots is maximal in that axis (see Fig. 1b). The effect of slots reduces the quantity of iron (especially in the d-axis) and thus the inductances computed using the actual model are lower than those obtained from the sinusoidal model but it approximates the measured value. The rest of the d-axis inductances are distributed amongst the cross-couplings as can be seen in Fig. 3. This difference is much lower in the q-axis. It is seen from the results that the average values of d-q-0 inductances calculated are very close to the experimental ones. High values of cross coupling effects exist which are usually not observed when approximate sinusoidal expressions are used. This is because all spurious harmonics are included in the calculations by using the actual geometry of the airgap and winding layout. The outlined procedure can be applied to other ac machines having a simple rotor configuration.

Acknowledgement

The author acknowledges the experience gained in 2006 while he was working on a five phase machine as a visiting research scholar with Dr. J. O. Ojo at Tennessee Technological University, Cookeville, USA under the sponsorship of Center for Energy Systems Research.

References

[1] Schimtz NL, Novotny DW. Introductory electromechanics. New York: The Ronald Press Company; 1950.
[2] Toliyat HA, Waikar SP, Lipo TA. Analysis and simulation of five-phase synchronous reluctance machines including third harmonic of airgap MMF. IEEE Trans Ind Appl 1998;34(2):332–9.
[3] Bianchi N. Electrical machines analysis using finite elements. Boca Raton: Taylor & Francis CRC; 2005.
[4] Joksimović MG, Durovic DM, Obradović BA. Skew and linear rise of mmf across slot modeling – winding function approach. IEEE Trans Energy Convers 1999;14(3):315–20.
[5] Lubin T, Hamiti T, Rezzoug A. Comparison between finite-element and winding function theory of inductances and torque calculation of a synchronous reluctance machine. IEEE Trans Magn 2007;43(8):3406–10.